

Electronic Supplementary Material (ESI) for New Journal of Chemistry.

Electronic Supplementary Information †

4,4'-Bipyridine-based Ni(II)-metallogel for fabricating a photo-responsive Schottky barrier diode device

Pubali Das,^a Santanu Majumdar,^b Arka Dey,^a Sourav Mandal,^b Atish Mondal,^b Sinchan Chakrabarty,^b Partha Pratim Ray,^{*,a} and Biswajit Dey^{*,b}

^aDepartment of Physics, Jadavpur University, Jadavpur, Kolkata, 700032, India.

^bDepartment of Chemistry, Visva-Bharati University, Santiniketan-731235, India.

*(B.D.) E-mail: bdeychem@gmail.com

*(PPR) E-mail: partha@phys.jdvu.ac.in

Table S1. Representative influence of the metal counter-anion on the gelation ability of the Ni-D-TA metallogel system.^a

Entry	Metal Salt	[Metal Salt]	[Ligand]	Vol. ^b	Phase ^c	Picture
1.	Ni(OAc) ₂ ·4H ₂ O	1 mM	1 mM	1 mL	S	
2.	Ni(NO ₃) ₂ ·6H ₂ O	1 mM	1 mM	1 mL	WG	
3.	NiSO ₄ ·6H ₂ O	1 mM	1 mM	1 mL	P	

^aGelation tests were performed as described in the Experimental Section. ^bTotal volume of solvent. ^cAbbreviations: S = solution, WG = weak gel, P = precipitate

Chemical response of Ni-D-TA metallogel towards different polar and non-polar solvents:

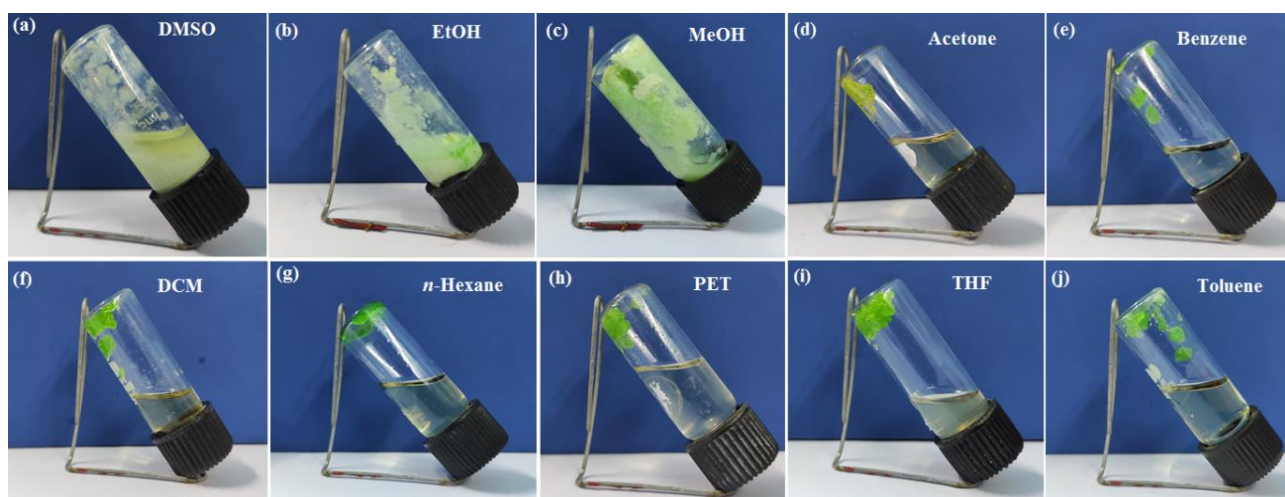


Fig. S1. Gelation process of Ni-D-TA metallogel in various solvents: precipitate for (a), (b) and (c) and insoluble for (d)-(j)

Exposure of ultra-sonication to Ni-D-TA metallogel:

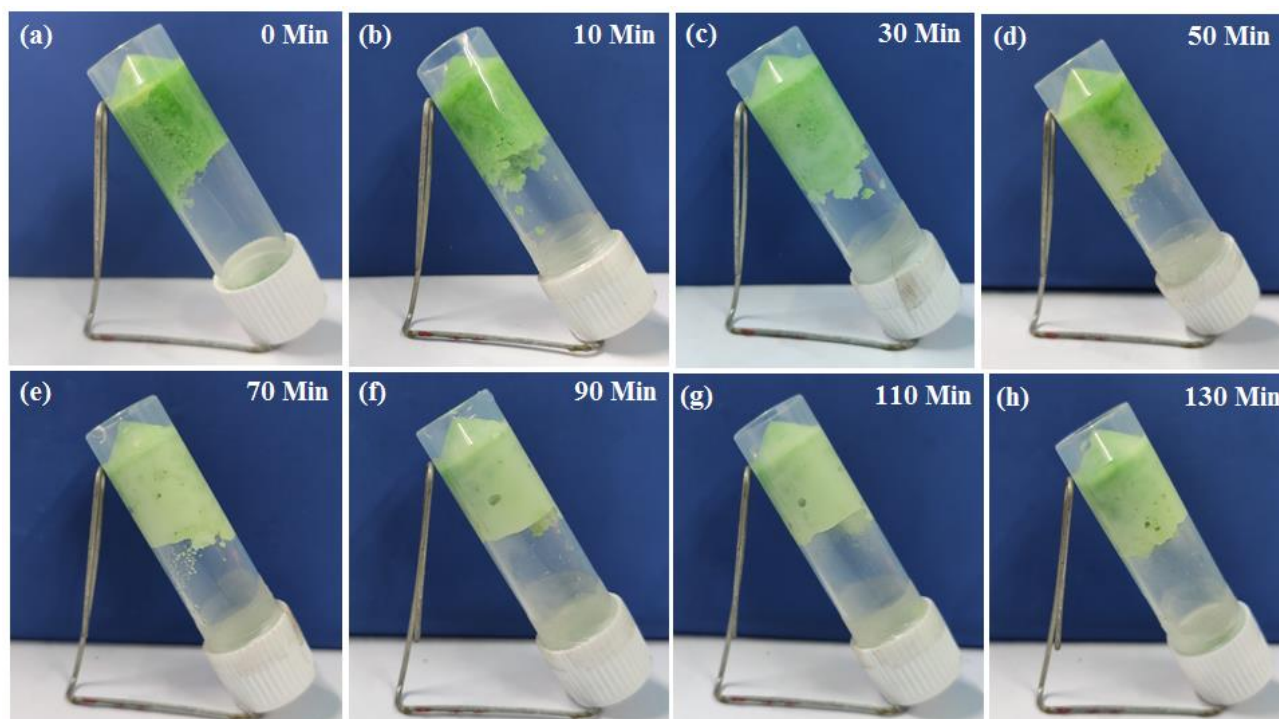


Fig. S2. Effect of ultra-sonication to Ni-D-TA metallogel from (a) initial to (h) 130 min of continuous ultra-sonication at 80 KHz.

Note: After allowing to stand (without any ultra-sonication condition) for ~30 min of each set, the metallogel was re-appeared to its initial status (as found in Figure S2 a) under ambient atmospheric condition.

Elemental Analysis:

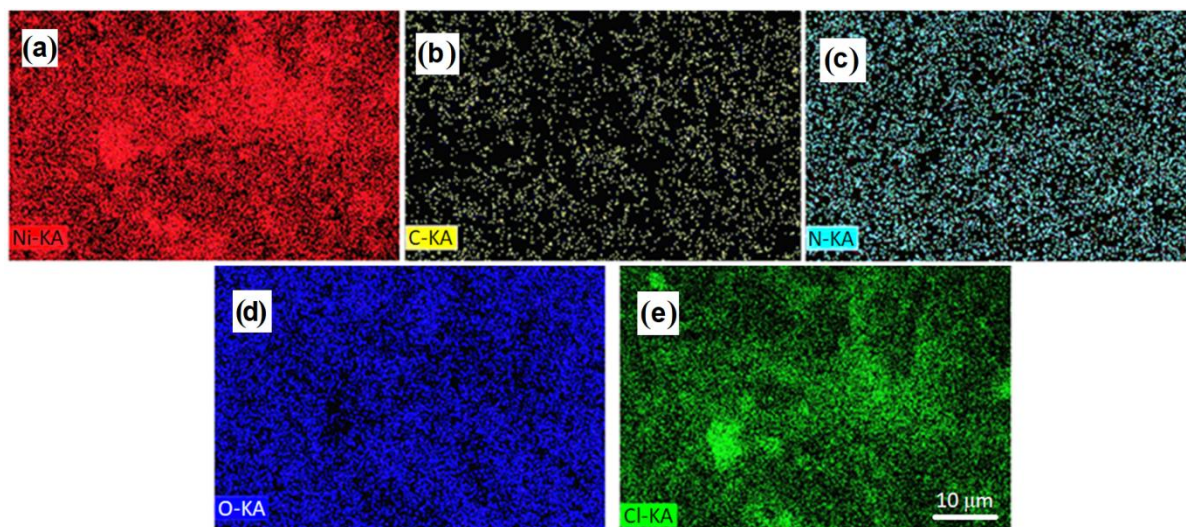


Fig. S3. The elemental mapping of Ni-D-TA showing the presence of (a) Ni, (b) C, (c) N, (d) O, and (e) Cl elements as the constitutions of the stable Ni-D-TA metallogel.

ESI-MS Analysis:

The metallogel-forming chemical association gets well-characterized by ESI-MS spectral analysis of the xerogel-form of the Ni(II)-metallogel (Fig. S4). Several peaks of the ESI-MS spectrum (Fig. S4) confirm the presences of different metallogel-forming constituents like triethylamine, 4,4'-dipyridyl, NiCl₂·6H₂O. Particularly, the marked peaks of the ESI-MS result represent the association of NiCl₂ and one 4,4'-dipyridyl, and the assembly of NiCl₂ and two 4,4'-dipyridyl units of Ni-D-TA metallogel. These two marked peaks of ESI-MS spectra also indicate the characteristic units that might be responsible to construct the stable gel-network of Ni-D-TA metallogel.

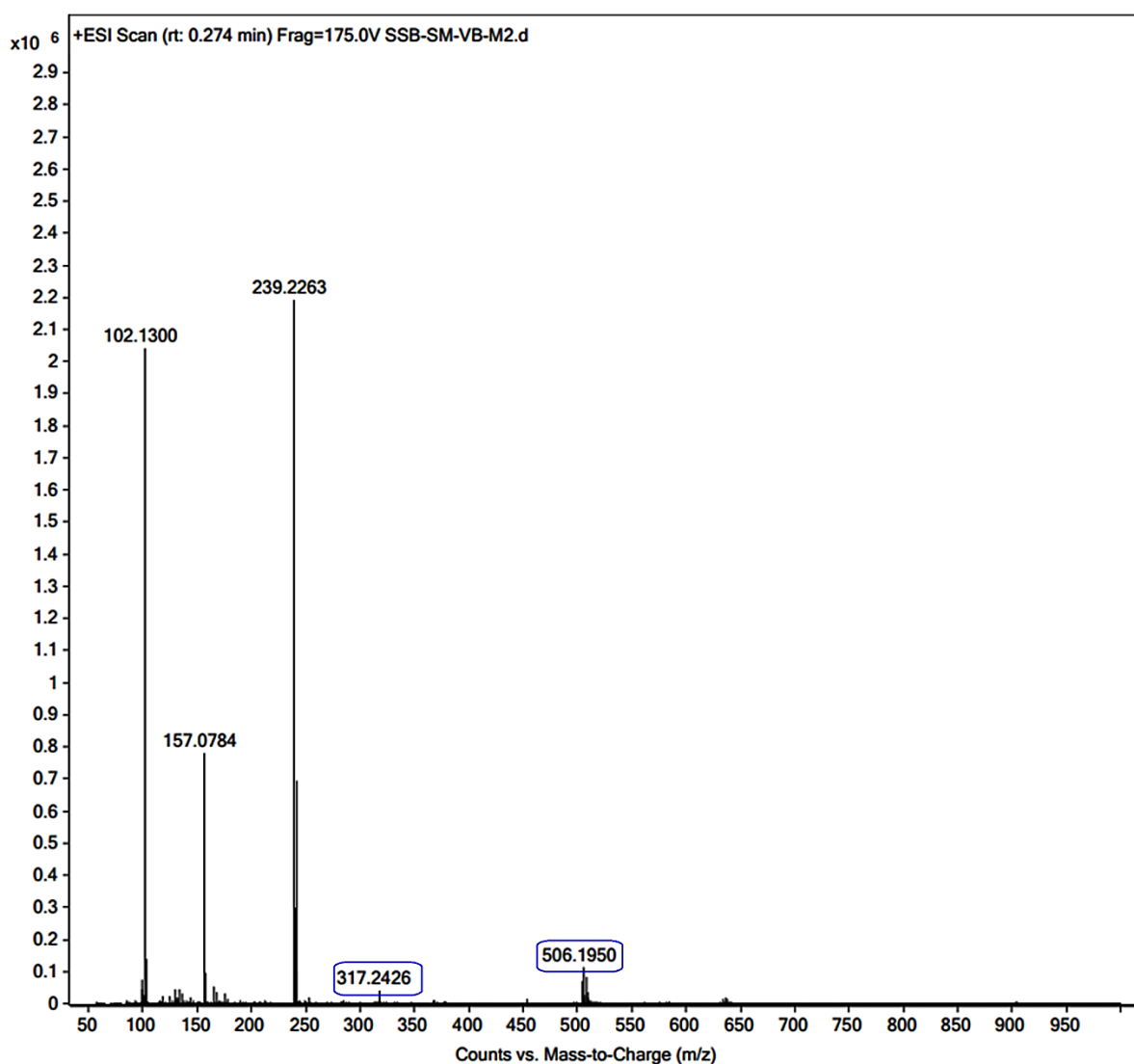


Fig. S4. ESI-MS of the xerogel of Ni-D-TA metallogel.

Powder X-Ray Diffraction Study:

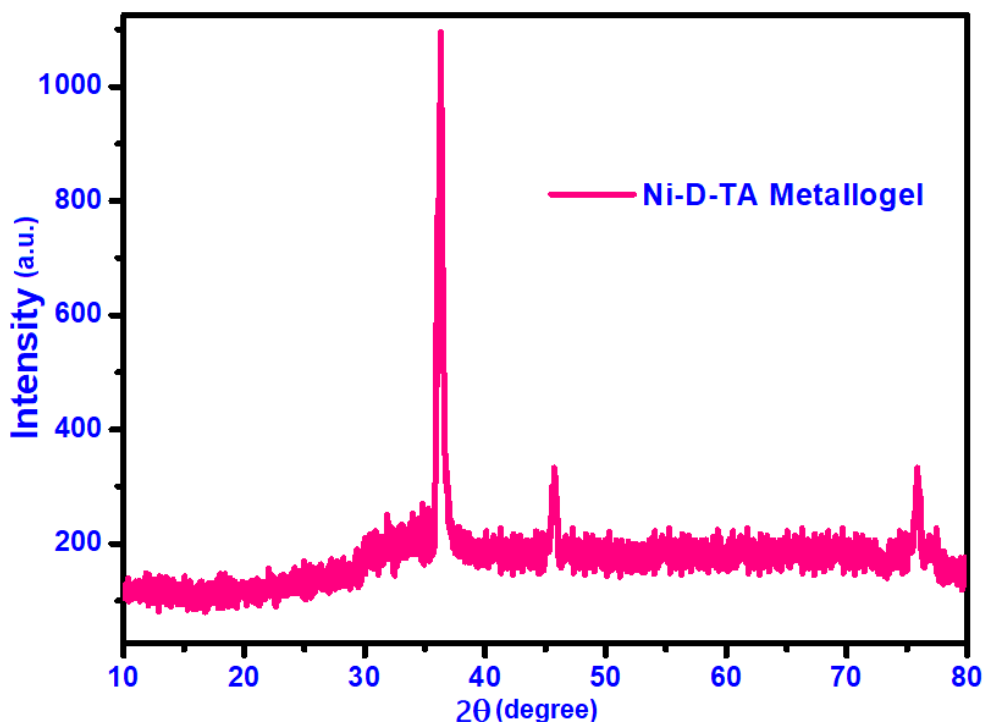


Fig. S5. PXRD pattern of Ni-D-TA metallogel.

The powder X-ray diffraction spectra of the Ni-D-TA metallogel has been recorded (Fig. S5). The PXRD data of Ni-D-TA metallogel shows that the semi-crystalline mixed-phase type material has been formed. The comparison of the experimental PXRD pattern of Ni-D-TA metallogel with the reported PXRD patterns of $\text{NiCl}_2 \cdot 6\text{H}_2\text{O}$ ¹ and 4,4'-dipyridyl² also supports towards formation of stable Ni-D-TA metallogel structure.

Optical Characterization

The optoelectronic property of our metallogel has been studied by UV-vis spectroscopy. The spectrum has been analyzed (inset of Fig. S6) within 300-900 nm. Employing equation S1 (Tauc's equation), estimation of optical band gap was done:³

$$(\alpha h\nu) = A(h\nu - E_g)^n \quad (\text{S1})$$

where, α , E_g , h and ν has their usual notation. In this equation there is an electron transition dependent constant ' n ' and another constant ' A ' which has value 1 for the ideal case. For direct allowed transition the value of n is $\frac{1}{2}$. Optical band gap (E_g) for direct transition has been estimated as 3.11 eV for our synthesized metallogel.

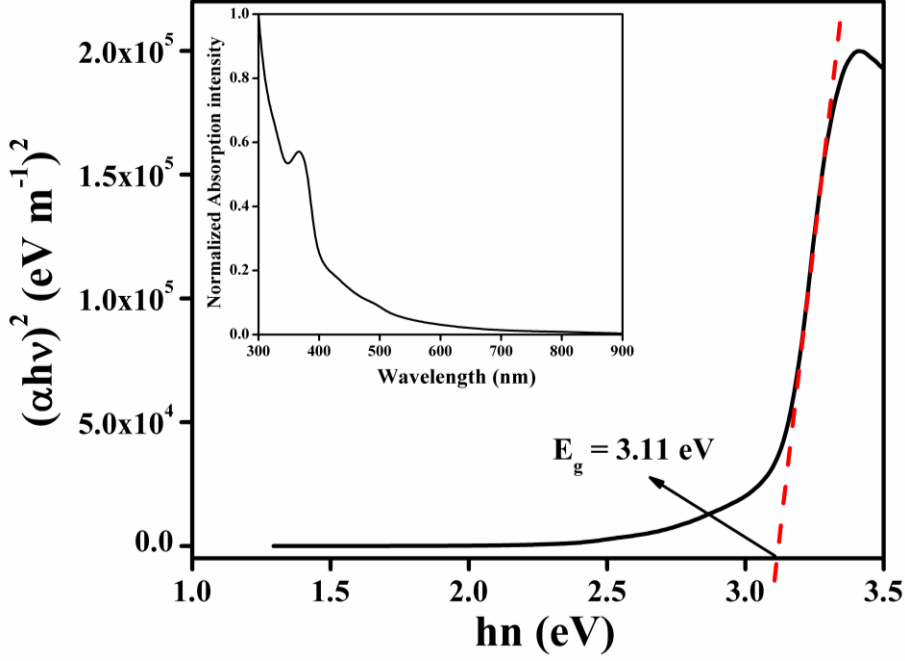


Fig. S6. UV-Vis absorption spectra (inset) and Tuac's plots for Ni-D-TA metallogel.

Device Fabrication

To perform the electrical analysis of our synthesized material we have developed multiple metal-semiconductor (MS) junction devices with the sandwich-like configuration of ITO/Ni-D-TA metallogel/Al. To fabricate the MS junction devices, thin film of as-synthesized Ni-D-TA metallogel was grown on precleaned ITO coated glass substrate by doctors blade method. Here we used aluminium, deposited on a plain glass slide in the Vacuum Coating Unit under base pressure 10^{-6} Torr as metal electrode.

Using Source-meter made by Keithley (model no: 2635B) and adopting two-probe technique, the current-voltage (I - V) characteristics of the devices was measured to analyze the electrical properties. All the device fabrication and measurements were carried out at room temperature and under ambient conditions.

Electrical Property Analysis

The I - V characteristic of the synthesized Ni-D-TA metallogel based Schottky diode (SD) has been further analyzed by thermionic emission theory. Cheung's method has also been employed to extract important diode parameters.³ In this regard, the obtained I - V curve has been analysed quantitatively by considering the following standard equations:^{3,4}

$$I = I_0 \exp\left(\frac{qV}{\eta KT}\right) \left[1 - \exp\left(\frac{-qV}{\eta KT}\right)\right] \quad (\text{S2})$$

$$I_0 = AA^* T^2 \exp\left(\frac{-q\phi_B}{KT}\right) \quad (\text{S3})$$

where I_0 , q , k , T , V , A , η and A^* stands for saturation current, electronic charge, Boltzmann constant, temperature in Kelvin, forward bias voltage, effective diode area, ideality factor and effective Richardson constant, respectively. The effective Richardson constant was considered as $32 \text{ AK}^{-2} \text{ cm}^{-2}$ for the fabricated devices.

The series resistance, ideality factor and barrier potential height was also determined by using equations S4 to S6, which was extracted from Cheung's idea,^{5,6}

$$\frac{dV}{d(\ln I)} = \left(\frac{\eta kT}{q}\right) + IR_S \quad (\text{S4})$$

$$H(I) = V - \left(\frac{\eta kT}{q}\right) \ln\left(\frac{I}{AA^*T^2}\right) \quad (\text{S5})$$

$$H(I) = IR_S + \eta\phi_B \quad (\text{S6})$$

The deviation from the ideal value of 1 can be attributed to the presence at the junction of Schottky inhomogeneities, interface defect states and/or series resistance.^{7,8} On the other side, better homogeneity for the Schottky barrier at the MS interface and the recombination of less charge carriers upon light irradiation would explain the lower values of η for our devices.³ This fact indicates that our devices possess lesser recombination of carriers at the interface, i.e., an improved barrier homogeneity, with light irradiation.

The effective carrier mobility (μ_{eff}) can be determined employing the Mott-Gurney equation (Equation S7) in the SCLC model with the high voltage data of the I vs. V^2 plot (Figure 8):^{3,6,9}

$$I = \frac{9\mu_{eff}\varepsilon_0\varepsilon_r A}{8} \left(\frac{V^2}{d^3}\right) \quad (\text{S7})$$

where, I , μ_{eff} , ε_r , and ε_0 are the current, the effective mobility, the relative dielectric constant of the material and the free space permittivity, respectively.

The dielectric constant of the material (ε_r) can be calculated from the saturation region of the capacitance vs. frequency curve at higher frequency (Figure 9) with the equation given below:³

$$\varepsilon_r = \frac{1}{\varepsilon_0} \cdot \frac{C d}{A} \quad (\text{S8})$$

where, C , d , and A are the capacitance at saturation, the thickness of the film ($\sim 1 \mu\text{m}$) and the device area, respectively. With this formula, we obtain ϵ_r values of 6.15×10^{-2} for our Ni-D-TA metallogel.

To study the charge transport behaviour through the junction, we have evaluated the value of transit time (τ) and diffusion length (L_D). The value of τ can be determined using equation (S9) from the slope of the I vs. V plot (Figure 4) in the SCLC region (region II).³

$$\tau = \frac{9\epsilon_0\epsilon_r A}{8d} \left(\frac{V}{I}\right) \quad (\text{S9})$$

$$\mu_{eff} = \frac{qD}{kT} \quad (\text{S10})$$

$$L_D = \sqrt{2D\tau} \quad (\text{S11})$$

where, D stands for diffusion coefficient that can be determined using Einstein-Smoluchowski equation (equation S10).³

Reference:

- (1) N.-D. Jaji, M. B. H. Othman, H. L. Lee, M. H. Hussin and D. Hui, *Nanotechnology Reviews*, 2021; **10**, 318-329.
- (2) M. A. Mohammad, A. Alhalaweh and S. P. Velaga, *International Journal of Pharmaceutics*, 2011, **407**, 63-71.
- (3) A. Dey, S. Middy, R. Jana, M. Das, J. Datta, A. Layek and P. P. Ray, *J. Mater. Sci.: Mater. Electron.*, 2016, **27**, 6325–6335.
- (4) E. H. Roderick, Oxford University Press, Oxford. 1978.
- (5) S. K. Cheung and N. W. Cheung, *Appl. Phys. Lett.*, 1986, **49**, 85–87.
- (6) A. Dey, A. Layek, A. Roychowdhury, M. Das, J. Datta, S. Middy, D. Das and P. P. Ray, *RSC Adv.*, 2015, **5**, 36560–36567.
- (7) R. K. Gupta, F. Yakuphanoglu, *Solar Energy.*, 2012, **86**, 1539–1545.
- (8) X. Miao, S. Tongay, M. K. Petterson, K. Berke, A. G. Rinzler, B. R. Appleton and A. F. Hebard, *Nano Lett.*, 2012, **12**, 2745–2750.
- (9) P. W. M. Blom, M. J. M. de Jong and M. G. van Munster, *Phys. Rev. B*, 1997, **55**, R656–R659.